Research Article

Ahmed E. Abouelregal, Hijaz Ahmad*, Mehmet Yavuz, Taher A. Nofal, and M. D. Alsulami

An orthotropic thermo-viscoelastic infinite medium with a cylindrical cavity of temperature dependent properties *via* MGT thermoelasticity

https://doi.org/10.1515/phys-2022-0143
received November 06, 2021; accepted March 31, 2022

Abstract: The current work is devoted to introduce a novel thermoelastic heat conduction model where the Moore-Gibson-Thompson (MGT) equation describes the heat equation. The constructed model is characterized by allowing limited velocities of heat wave propagation within the material, consistent with physical phenomena. The Green–Naghdi Type III model is improved by introducing the delay factor into the modified Fourier law. Also, from the presented model, some other models of thermoelasticity can be derived at specific states. Based on the suggested model, an infinite orthotropic material with a cylindrical hole exposed to time-dependent temperature variation was studied. It has also been considered that the coefficient of thermal conductivity varies with temperature, unlike in many other cases where this value is considered constant. The viscoelastic material of the investigated medium was assumed to be of the Kelvin–Voigt type. The Laplace transform method provides general solutions to the studied field variables equations. The effects of viscosity and thermal variability parameters on these fields are discussed and graphically presented. In addition, the numerical results were presented in tables, and a comparison with previous models was made to ensure the accuracy of the results of the proposed model.

Keywords: thermo-viscoelasticity, orthotropic material, cylindrical cavity, variable thermal conductivity, MGT heat equation

1 Introduction

The paradox of physical phenomena involving the transmission of heat waves at infinite speed appears in the classical theory of heat conduction, meaning that thermal disturbance is immediately felt throughout the physical body from the point of application. Several improvements have been proposed over the past decades to remedy this defect and allow limited velocities of heat wave propagation. Biot [1] proposed the dynamic coupled theory of thermal elasticity based on classical Fourier laws, but the governing equations in this theory are of the parabolic and hyperbolic types and thus allow the propagation of heat waves at unlimited speeds. For this reason, several generalized thermoelastic theories have been presented in recent years.

One of the first famous theories that emerged in this context to remove the shortcomings in the Biot theory was Lord and Schulman's [2] generalized theory, taking into account the Cattaneo–Vernotte modification of the heat equation [3–5]. By introducing the concept of relaxation time coefficient into the heat flow vector, Cattaneo–Vernotte introduced a modified form of Fourier's law as follows:

$$\left(1 + \tau_0 \frac{\partial}{\partial t}\right)\vec{q}(\vec{x}, t) = -K\vec{\nabla}\theta(\vec{x}, t), \tag{1}$$

where $\vec{q}$ indicates the vector of the heat flow, K indicates the thermal conductivity, $\theta = T - T_0$ indicates the temperature change, and τ_0 is the relaxation time coefficient.

* **Corresponding author: Hijaz Ahmad,** Section of Mathematics, International Telematic University Uninettuno, Corso Vittorio Emanuele II, 39, 00186 Roma, Italy, e-mail: hijaz555@gmail.com
Ahmed E. Abouelregal: Department of Mathematics, College of Science and Arts, Jouf University, Al-Qurayat, Saudi Arabia; Department of Mathematics, Faculty of Science, Mansoura University, Mansoura 35516, Egypt
Mehmet Yavuz: Department of Mathematics and Computer Sciences, Faculty of Science, Necmettin Erbakan University, 42090 Konya, Turkey
Taher A. Nofal: Department of Mathematics, College of Science, Taif University, P.O. Box 11099, Taif 21944, Saudi Arabia
M. D. Alsulami: Department of Mathematics, College of Sciences and Arts at Alkamil, University of Jeddah, Jeddah, Saudi Arabia

Some other theories in response to thermoelasticity were developed without there being any modifications to the classical Fourier law, as in refs [6–8]. In many books and articles, some of the pioneering achievements made by many researchers in this context have been written down, for example in refs [9–14]. Among the well-known theories that have spread widely in this field are those presented by Green and Naghdi [15]. The three theories developed by Green and Naghdi are classified as GN-I, GN-II, and GN-III types. In addition to the aforementioned and other efforts, some other efforts have been made to improve upon the classical Fourier law, such as those models adopted by Abouelregal [16–20] that include higher-order time derivatives.

According to the improved GN-III model, the Fourier law becomes

$$\vec{q}(\vec{x}, t) = -[K\vec{\nabla}\theta(\vec{x}, t) + K^*\vec{\nabla}\vartheta(\vec{x}, t)], \tag{2}$$

where $\dot{\vartheta} = \theta$ and K^* is the conductivity rate.

Note that when $K^* = 0$, we retrieve e and Naghdi model (GN-I), and the second type (GN-II) can also be acquired when the term containing the parameter K is neglected.

The equation of energy can be expressed as [10]

$$\rho C_E \frac{\partial\theta}{\partial t} + T_0\frac{\partial}{\partial t}(\beta_{ij}e_{ij}) = -q_{i,i} + Q, \tag{3}$$

where C_E denotes the specific heat, $\beta_{ij} = c_{ijkl}\alpha_{kl}$ is the thermal coupling coefficient, α_{kl} is the tensor of the thermal expansion coefficients, c_{ijkl} is the elastic coefficient, e_{ij} denotes the components of the strain tensor, Q represents the heat source, and ρ represents the density.

The combination of Eqs. (1) and (3) leads to a heat conduction equation of the kind that has physical defects propagated by the thermal signal with infinite velocity. Studies have proven that the improved Fourier law (2) leads to the same defects as in the usual theory of thermal elasticity, where it predicts the instantaneous propagation of thermal conduction waves. Also, in the GN-III model, the principle of causation was not taken into account. To address this defect in the classical and GN-III thermoelastic theories, a modified thermoelastic model was developed in which the heat conduction equation included a relaxation factor [21].

In recent years, the Moore-Gibson-Thompson (MGT) equation has been well received by many researchers due to its many applications. The MGT equation is a third-order partial differential equation, and one of its most important applications is used in many fluid dynamics issues as well as viscoelasticity [22]. This equation may also be produced by adding a relaxation factor to the Green–Naghdi model of type III heat conduction model, which was initially proposed in the framework of fluid mechanics. Quintanilla [21] has derived a novel type of thermoelastic conduction based on the MGT equation. As a result, it has recently been established as the thermal transfer equation. It may also be calculated as a special version of Choudhuri's three-phase-lag model [23]. Since the advent of MGT, the number of papers devoted to this theory has increased significantly [22–27]. The modified heat equation proposed by Quintanilla [21] can be expressed as

$$\vec{q}(\vec{x}, t) + \tau_0\frac{\partial\vec{q}(\vec{x}, t)}{\partial t} = -K\vec{\nabla}\theta(\vec{x}, t) - K^*\vec{\nabla}\vartheta(\vec{x}, t). \tag{4}$$

When Eqs. (3) and (4) are coupled, the MGT heat transfer equation can be obtained as [21,28]

$$\left(1 + \tau_0\frac{\partial}{\partial t}\right)\left[\frac{\partial}{\partial t}\left(\rho C_E\frac{\partial\theta}{\partial t}\right) + T_0\frac{\partial^2}{\partial t^2}(\beta_{ij}e_{ij}) - \frac{\partial Q}{\partial t}\right] = \nabla.(K\nabla\dot{\theta}) + \nabla.(K^*\nabla\theta). \tag{5}$$

The modified MGTE theory is a generalization of Lord–Shulman's theory (LS) [2] and the GN-III model of thermoelasticity [16]. Based on this modified model, many problems of fluid mechanics as well as thermal and mechanical behavior of many engineering structures have been studied in recent years [29–36].

Viscoelasticity is the quality of materials that display viscoelastic and elastic qualities when distorted, as defined in materials engineering and continuity mechanics. When pressure is applied to viscous materials, such as water, they resist shear and pressure flow linearly over time. When elastic materials are stretched, they expand and then return to their original status when the force is removed. A viscoelastic material has both an elastic and a viscous element, as opposed to solely elastic substances. A viscoelastic substance's viscosity causes it to have a time-dependent strain rate. When a thermal or mechanical load is employed and then withdrawn, pure elastic materials do not lose energy (heat). When a load is applied and then withdrawn, however, a viscoelastic medium dissipates energy. The Kelvin–Voigt model, commonly known as the Voigt model, may be described by a completely viscous damper and a purely elastic spring coupled in parallel. The Kelvin–Voigt model is depicted schematically. Instead, we may make a model of a Maxwell substance by connecting these two parts in a series.

In many applications, various investigations of generalized thermoelastic problems as well as those

associated with viscoelastic thermal problems have been discussed. Kovalenko and Karnaukhov [37] presented the widely spread linear thermo-viscosity theory, including the effect of thermogenesis. For the non-isothermal viscous activity of polymers on finite strains, Drozdov [38] constructed its basic equations. Alharbi and Bayones [39] studied the effect on the spreading of Rayleigh waves in a thermoelastic viscous, elastic, and homogeneous materials under the influence of magnetic field, rotation, and primary pressure. In the field of viscoelasticity and thermal viscoelasticity, many applications have been presented in various fields, whether engineering or physical [41–45]. The hygrothermal study looks at how heat, air, and moisture travel inside building enclosures (walls, roofs, floors, and below-grade). Temperature, humidity, and moisture content data from materials and surfaces throughout the assembly are included in the outputs of the hygrothermal model. There is a large body of knowledge focusing on the hygrothermal effects of the mechanical properties of composite films, among others [46–52].

Some physical properties in thermoplastic elastomers and materials are highly dependent on temperature change. Many problems are concerned with the study of elastic materials without taking into account the change in thermal conductivity with the change in temperature. Thermal conductivity is so significant in many fields of structural, biochemical, industrial, and other applications, particularly if it is affected by temperature changes. This is one of the reasons for presenting the current work.

Thermal stresses play a vital role in the construction of nuclear reactors, aircraft, stream turbines, missiles, internal combustion turbines, high-pressure gas compressors, rotating internal combustion engines, and other heat transfer machines. For example, in modern nuclear reactors and high-energy particle accelerators, the complex interaction between thermal and mechanical fields in solids is one of the practical applications of this presented work. Also, one of the most important things designers need to know when studying the strength of a material affected by temperature change is the distribution of the stresses, especially if the material's conductivity coefficient changes with temperature.

The main objective of the current study is to investigate the effect of changing the thermal conductivity on a viscoelastic elastic medium. The thermo-viscosity interactions of this medium, which have been studied is within the framework of a novel generalized thermoelastic model based on the MGT equation. This proposed generated model is based on the Quintanilla [21] modification involving a relaxation time. In addition, this new model addresses the shortcomings of the type III Green–Naghdi model, which predicts unlimited speeds like the classical theory. The Kelvin–Voigt type is considered, which is one of the most widely used mechanical models to study the behavior of viscoelastic materials.

The presented model was used to study a viscous thermoelastic medium with an infinite cylindrical cavity. The inner surface of the cylindrical cavity was assumed to be stress-free and thermally loaded. The fundamental equations of the system were solved by applying the Laplace transform method. The numerical results of all the physical quantities are discussed theoretically and graphically. Some special cases are explained in which the viscosity coefficient is negligible and the coefficient of thermal conductivity is constant.

The additional governing equations can be expressed as [52,53]

$$\sigma_{ij} = \left(1 + t_0 \frac{\partial}{\partial t}\right)(c_{ijkl} e_{kl} - \beta_{ij}\theta), \tag{6}$$

$$e_{ij} = \frac{1}{2}(u_{j,i} + u_{i,j}), \tag{7}$$

$$\sigma_{ij,j} = \rho \frac{\partial^2 u_i}{\partial t^2}, \tag{8}$$

where σ_{ij} is the stress tensor and u_i denote the displacement components.

2 Problem formulation

At a constant reference temperature T_0, the behavior of an infinite cylindrical hole, viscous, anisotropic elastic body will be studied. It was assumed that the inner surface of the cylindrical cavity was free of traction and subjected to a time-dependent temperature shock. The Kelvin–Voigt linear viscosity model was also used to determine the viscoelastic behavior and properties of the material. To discuss the problem, the cylindrical coordinate system (r, ξ, z) was used, where z represents the axial coordinate of the cylinder. It is considered that the disturbances are finite and confined to a region close to the interface $r = R$, and disappear as $r \to \infty$.

As a result of the axial symmetry of the cylinder, the components of the non-vanishing strain displacement are as follows:

$$u_r = u(r, t), \quad u_\xi(r, t) = u_z(r, t) = 0, \tag{9}$$

$$e_{rr} = \frac{\partial u}{\partial r}, \quad e_{\xi\xi} = \frac{u}{r}, \quad e_{r\xi} = e_{rz} = e_{z\xi} = 0. \tag{10}$$

The constituent relationships of the Kelvin–Voigt viscoelastic type takes the form [53]

$$[\sigma_{rr},\ \sigma_{\xi\xi},\ \sigma_{zz}]^{T_r} = \tau_m \begin{bmatrix} c_{11} & c_{12} & \beta_{11} \\ c_{12} & c_{22} & \beta_{22} \\ c_{13} & c_{23} & \beta_{33} \end{bmatrix} \left[\frac{\partial u}{\partial r},\ \frac{u}{r},\ -\theta \right]^{T_r}, \quad (11)$$

where $\tau_m = 1 + t_0 \frac{\partial}{\partial t}$. The dynamic Eq. (8) can be expressed in cylindrical coordinates as

$$\frac{\partial \sigma_{rr}}{\partial r} + \frac{1}{r}(\sigma_{rr} - \sigma_{\xi\xi}) = \rho \frac{\partial^2 u}{\partial t^2}. \quad (12)$$

After using Eq. (11), the equation of motion (12) can be expressed as

$$\begin{aligned} &\tau_m c_{11}\left(\frac{\partial}{\partial r} + \frac{1}{r}\right)\left(\frac{\partial u}{\partial r}\right) - \tau_m c_{22}\frac{u}{r^2} \\ &= \tau_m \beta_{11}\frac{\partial \theta}{\partial r} + \tau_m(\beta_{11} - \beta_{22})\frac{\theta}{r} + \rho\frac{\partial^2 u}{\partial t^2}. \end{aligned} \quad (13)$$

In the cylindrical coordinates, the heat conduction MGT Eq. (5) reduces to [21,28]

$$\begin{aligned} &\left(1 + \tau_0 \frac{\partial}{\partial t}\right)\left[\frac{\partial}{\partial t}\left(\rho C_E \frac{\partial \theta}{\partial t}\right) + T_0 \frac{\partial^2}{\partial t^2}\left(\beta_{11}\frac{\partial u}{\partial r} + \beta_{22}\frac{u}{r}\right)\right] \\ &= \frac{\partial}{\partial t}[\nabla.\ (K\nabla\theta)] + \frac{\partial}{\partial t}[\nabla.\ (K^* \quad \nabla\vartheta)]. \end{aligned} \quad (14)$$

3 Temperature dependence of thermal conductivity

In general, the thermal conductivity of materials k is often a function of temperature change. Also, depending on the type of material, the form of functional dependence varies. In this work, we will take into account that the thermal conductivity and the specific heat coefficient C_E are linear functions of the temperature change in the following form [54]:

$$\begin{aligned} K &= K(\theta) = K_0(1 + K_1\theta), \\ C_E &= C_E(\theta) = C_{E0}(1 + K_1\theta), \end{aligned} \quad (15)$$

where K_0, C_{E0}, and K_1 are constants. From the previous relationship, it can be seen that the diffusion coefficient k, $(k = K/(\rho C_E))$ is a constant. It is also noted that when the coefficient of change of thermal conductivity vanishes $(K_1 = 0)$, the coefficient of thermal conductivity and the specific heat of the material becomes constant.

On the same approach, we will take into account that the rate of thermal conductivity K^* changes with the change in temperature according to the following relationship:

$$K^* = K^*(\theta) = K_0^*(1 + K_2\vartheta), \quad (16)$$

where K_0^* and K_2 are constants. After using Eqs. (15) and (16), the conduction Eq. (14) becomes a nonlinear partial differential equation of the following form:

$$\begin{aligned} &\left(1 + \tau_0\frac{\partial}{\partial t}\right)\left[\frac{\partial}{\partial t}\left(\rho C_E\frac{\partial\theta}{\partial t}\right) + T_0\frac{\partial^2}{\partial t^2}\left(\beta_{11}\frac{\partial u}{\partial r} + \beta_{22}\frac{u}{r}\right)\right] \\ &= K_0\frac{\partial}{\partial t}[\nabla.\ ((1 + K_1\theta)\nabla\theta)] \\ &\quad + K_0^*\frac{\partial}{\partial t}[\nabla\cdot((1 + K_2\vartheta)\nabla\vartheta)]. \end{aligned} \quad (17)$$

The following Kirchhoff transformation can be used to simplify the above equation into linear form [48]

$$\begin{aligned} \psi_1 &= \int_0^\theta (1 + K_1\varphi)\mathrm{d}\varphi, \\ \psi_2 &= \int_0^\vartheta (1 + K_2\varphi)\mathrm{d}\varphi. \end{aligned} \quad (18)$$

After entering Eq. (13) in Eq. (14) and integrating, we can obtain [55]

$$\begin{aligned} \psi_1 &= \theta\left(1 + \tfrac{1}{2}K_1\theta\right), \\ \psi_2 &= \vartheta\left(1 + \tfrac{1}{2}K_2\vartheta\right). \end{aligned} \quad (19)$$

From the relations given in Eq. (18), we can conclude that

$$\begin{aligned} &\frac{K(\theta)}{K_0}\nabla\theta = \nabla\psi_1, \quad \frac{K^*(\theta)}{K_0^*}\nabla\theta = \nabla\psi_2, \\ &\frac{K}{K_0}\frac{\partial\theta}{\partial t} = \frac{\partial\psi_1}{\partial t}, \quad \frac{\partial\psi_2}{\partial t} = \frac{K^*}{K_0^*}\frac{\partial\vartheta}{\partial t} = \frac{K^*}{K_0^*}\theta. \end{aligned} \quad (20)$$

Differentiating Eq. (20) again with respect to the distances, we have

$$\begin{aligned} \nabla.\left(\frac{K(\theta)}{K_0}\nabla\theta\right) &= \nabla^2\psi_1, \\ \nabla.\left(\frac{K^*(\theta)}{K_0^*}\nabla\theta\right) &= \nabla^2\psi_2. \end{aligned} \quad (21)$$

Using the relation $|\theta/T_0| \ll 1$, where $\theta = T - T_0$, we can conclude that:

$$\frac{\partial}{\partial t}\nabla^2\psi_2 \approx K^*\nabla^2\psi_1. \quad (22)$$

Using the above relations, the nonlinear heat conduction Eq. (18) can be transformed into the following linear form

$$\left(1+\tau_0\frac{\partial}{\partial t}\right)\left[\frac{1}{k}\frac{\partial\psi_1}{\partial t}+\frac{T_0}{K_0}\frac{\partial^2}{\partial t^2}\left(\beta_{11}\frac{\partial u}{\partial r}+\beta_{22}\frac{u}{r}\right)\right] = \frac{\partial}{\partial t}\nabla^2\psi_1+\frac{K_0^*}{K_0}\nabla^2\psi_1. \tag{23}$$

The equation of motion (13) can also be derived in the following non-linear form

$$\tau_m c_{11}\left(\frac{\partial^2 u}{\partial r^2}+\frac{1}{r}\frac{\partial u}{\partial r}\right)-\tau_m c_{22}\frac{u}{r^2} = \frac{\tau_m\beta_{11}}{1+K_1\theta}\frac{\partial\psi_1}{\partial r}+\frac{\tau_m(\beta_{11}-\beta_{22})}{K_1 r} (-1+\sqrt{1+2K_1\psi_1})+\rho\frac{\partial^2 u}{\partial t^2}. \tag{24}$$

For linearity, $|\theta/T_0|\ll 1$, where $\theta = T - T_0$, then we have

$$\tau_m c_{11}\left(\frac{\partial^2 u}{\partial r^2}+\frac{1}{r}\frac{\partial u}{\partial r}\right)-\tau_m c_{22}\frac{u}{r^2} = \frac{\beta_{11}}{1+K_1\theta}\frac{\partial\psi_1}{\partial r}+(\beta_{11}-\beta_{22})\frac{\psi_1}{r}+\rho\frac{\partial^2 u}{\partial t^2}, \tag{25}$$

$$\begin{bmatrix}\sigma_{rr}\\ \sigma_{\xi\xi}\\ \sigma_{zz}\end{bmatrix} = \tau_m\begin{bmatrix}c_{11} & c_{12} & -\beta_{11}\\ c_{12} & c_{22} & -\beta_{22}\\ c_{13} & c_{23} & -\beta_{33}\end{bmatrix}\begin{bmatrix}\frac{\partial u}{\partial r}\\ \frac{u}{r}\\ \psi_1\end{bmatrix}. \tag{26}$$

We will apply the dimensionless variables listed below for convenience

$$\{u', r', R'\} = \frac{c_0}{k}\{u, r, R\},\quad \{t', \tau_0'\} = \frac{c_0^2}{k}\{t, \tau_0\},\quad \theta' = \frac{\theta}{T_0},\quad \sigma_{ij}' = \frac{\sigma_{ij}}{c_{11}},\quad K_1' = T_0K_1,\quad c_0^2 = \frac{c_{11}}{\rho}. \tag{27}$$

We can get the following by suppressing the dashes and then using the variables of Eq. (27) in Eqs. (23), (25), and (26)

$$\tau_m\left(\frac{\partial^2 u}{\partial r^2}+\frac{1}{r}\frac{\partial u}{\partial r}\right)-\tau_m c_2\frac{u}{r^2} = \varepsilon_1\frac{\partial\psi_1}{\partial r}+\varepsilon_0\frac{\psi_1}{r}+\frac{\partial^2 u}{\partial t^2}, \tag{28}$$

$$\left(1+\tau_0\frac{\partial}{\partial t}\right)\left[\frac{\partial^2\psi_1}{\partial t^2}+\frac{\partial^2}{\partial t^2}\left(\varepsilon_4\frac{\partial u}{\partial r}+\varepsilon_5\frac{u}{r}\right)\right] = \frac{\partial}{\partial t}\nabla^2\psi_1+\omega\nabla^2\psi_1, \tag{29}$$

$$\begin{bmatrix}\sigma_{rr}\\ \sigma_{\xi\xi}\\ \sigma_{zz}\end{bmatrix} = \tau_m\begin{bmatrix}1 & c_1 & -\varepsilon_1\\ c_1 & c_2 & -\varepsilon_2\\ c_3 & c_4 & -\varepsilon_3\end{bmatrix}\begin{bmatrix}\frac{\partial u}{\partial r}\\ \frac{u}{r}\\ \psi_1\end{bmatrix}, \tag{30}$$

where

$$c_1=\frac{c_{12}}{c_{11}},\quad c_2=\frac{c_{22}}{c_{11}},\quad c_1=\frac{c_{13}}{c_{11}},\quad c_1=\frac{c_{23}}{c_{11}},\quad \varepsilon_1=\frac{T_0\beta_{11}}{c_{11}},\quad \varepsilon_2=\frac{T_0\beta_{22}}{c_{11}},\quad \varepsilon_3=\frac{T_0\beta_{33}}{c_{11}},\quad \varepsilon_4=\frac{\beta_{11}}{\rho C_E},\quad \varepsilon_5=\frac{\beta_{22}}{\rho C_E},\quad \varepsilon_0=\frac{T_0(\beta_{11}-\beta_{22})}{c_{11}},\quad \omega=\frac{K_0^*}{c_0^2K_0}. \tag{31}$$

4 Conditions of the problem

We will assume that in the beginning, the matter was in a state of rest, and therefore the initial conditions can be imposed as follows:

$$u(r,t)|_{t=0} = 0 = \left.\frac{\partial u(r,t)}{\partial t}\right|_{t=0},\quad \theta(r,t)|_{t=0} = 0 = \left.\frac{\partial\theta(r,t)}{\partial t}\right|_{t=0},\quad \psi_1(r,t)|_{t=0} = 0 = \left.\frac{\partial\psi_1(r,t)}{\partial t}\right|_{t=0}, \tag{32}$$

$$u(r,t) = \theta(r,t) = \psi_1(r,t) = 0 \text{ at } r\to\infty. \tag{33}$$

To address the proposed problem, it will be assumed that the inner surface of the cylinder is treated with thermal shock, time-dependent and traction-free. Thus, the boundary conditions imposed on the problem are as follows:

$$\theta(r,t) = \theta_0 H(t) \text{ at } r = a, \tag{34}$$

where the parameter θ_0 is fixed

$$\sigma_{rr}(r,t) = 0 \text{ at } r = a. \tag{35}$$

After applying Eq. (18), we have

$$\psi_1(r,t) = \theta_0 H(t)+\frac{K_1}{2}(\theta_0 H(t))^2 \text{ at } r = a. \tag{36}$$

5 Laplace transform method

To solve the basic equations, the Laplace transform method will be used on Eqs. (28)–(30), taking into account the initial conditions (32)

$$\bar{\tau}_m\left(\frac{\mathrm{d}^2\bar{u}}{\mathrm{d}r^2}+\frac{1}{r}\frac{\mathrm{d}\bar{u}}{\mathrm{d}r}\right)-\bar{\tau}_m\frac{\bar{u}}{r^2}-s^2\bar{u} = \bar{\tau}_m\varepsilon_1\frac{\mathrm{d}\bar{\psi}_1}{\mathrm{d}r}, \tag{37}$$

$$s^2\bar{\psi}_1 + \varepsilon\bar{\tau}_m s^2\left(\frac{\mathrm{d}\bar{u}}{\mathrm{d}r} + \frac{\bar{u}}{r}\right) = \frac{(s+\omega)}{(1+\tau_0 \quad s)}\nabla^2\bar{\psi}_1, \tag{38}$$

$$\begin{bmatrix}\sigma_{rr}\\ \sigma_{\xi\xi}\\ \sigma_{zz}\end{bmatrix} = \begin{bmatrix}\bar{\tau}_m & \bar{\tau}_m c_1 & -\varepsilon_1\\ \bar{\tau}_m c_1 & \bar{\tau}_m c_2 & -\varepsilon_1\\ \bar{\tau}_m c_3 & \bar{\tau}_m c_4 & -\varepsilon_3\end{bmatrix}\begin{bmatrix}\dfrac{\mathrm{d}\bar{u}}{\mathrm{d}r}\\ \dfrac{\bar{u}}{r}\\ \bar{\psi}_1\end{bmatrix}, \tag{39}$$

where $\beta_{11} = \beta_{22}$ ($\varepsilon_4 = \varepsilon_5 = \varepsilon, \quad \varepsilon_0 = 0$), $c_{11} = c_{22}$, and $\bar{\tau}_m = 1 + t_0 s$.

Eqs. (37) and (38) can be reformulated as follows:

$$\left(DD_1 - \frac{s^2}{\bar{\tau}_m}\right)\bar{u} = \frac{\varepsilon_1}{\bar{\tau}_m}\frac{\mathrm{d}\bar{\psi}_1}{\mathrm{d}r}, \tag{40}$$

$$\varepsilon q\bar{\tau}_m D_1\bar{u} = (D_1 D - q)\bar{\psi}_1, \tag{41}$$

where

$$D = \frac{\mathrm{d}}{\mathrm{d}r}, \quad D_1 = \frac{\mathrm{d}\bar{u}}{\mathrm{d}r} + \frac{\bar{u}}{r}, \quad q = \frac{s^2(1+\tau_0 \quad s)}{(s+\omega)}. \tag{43}$$

Defining a new function often called the thermoelastic potential function ϕ, which is as follows

$$u = \frac{\mathrm{d}\phi}{\mathrm{d}r}, \tag{44}$$

Eqs. (40) and (41) can be expressed as

$$\left(D_1 D - \frac{s^2}{\bar{\tau}_m}\right)\bar{\phi} = \frac{\varepsilon_1}{\bar{\tau}_m}\bar{\psi}_1, \tag{45}$$

$$\varepsilon q\bar{\tau}_m D_1 D\bar{\phi} = (D_1 D - q)\bar{\psi}_1. \tag{46}$$

From Eqs. (45) and (46), we obtain

$$\left((D_1 D)^2 - \left(q + \frac{s^2}{\bar{\tau}_m} + \frac{\varepsilon q\varepsilon_1}{\bar{\tau}_m}\right)(D_1 D) + \frac{qs^2}{\bar{\tau}_m}\right)\bar{\phi} = 0. \tag{47}$$

Eq. (47) can be rewritten as

$$(\nabla^2 - m_1^2)(\nabla^2 - m_2^2)\bar{\phi} \quad = 0, \tag{48}$$

where the parameters m_1^2 and m_2^2 satisfy the following relation

$$m^2 - \left(q + \frac{s^2}{\bar{\tau}_m} + \frac{\varepsilon q\varepsilon_1}{\bar{\tau}_m}\right)m + \frac{qs^2}{\bar{\tau}_m} = 0, \tag{49}$$

where

$$A = q + \frac{s^2}{\bar{\tau}_m} + \frac{\varepsilon q\varepsilon_1}{\bar{\tau}_m}, \quad B = \frac{qs^2}{\bar{\tau}_m}, \quad \nabla^2 = \frac{\partial^2}{\partial r^2} + \frac{1}{r}\frac{\partial}{\partial r}. \tag{50}$$

Under the assumptions of regularity, the solutions of Eq. (48) can be described as

$$\bar{\phi} = \sum_{i=1}^{2} A_i K_0(m_i r), \tag{51}$$

where $K_0(m_i r)$ denotes the modified Bessel function. Also, parameters A_i, $i = 1, 2$ represent the integral parameters. Introducing Eq. (51) in Eqs. (44) and (40), we get

$$\bar{\psi}_1 = \frac{\bar{\tau}_m}{\varepsilon_1}\sum_{i=1}^{2}\left(m_i^2 - \frac{s^2}{\bar{\tau}_m}\right)A_i K_0(m_i r), \tag{52}$$

$$\bar{u} = -\sum_{i=1}^{2} m_i A_i K_1(m_i r). \tag{53}$$

With the aid of the following relations

$$xK'_n(x) = -xK_{n+1}(x) + nK_n(x), \tag{54}$$

then the thermal stresses are given by

$$\bar{\sigma}_{rr} = \bar{\tau}_m\sum_{i=1}^{2}\left[\frac{s^2}{\bar{\tau}_m}A_i K_0(m_i r) + \frac{m_i(1-c_1)}{r}A_i K_1(m_i r)\right], \tag{55}$$

$$\bar{\sigma}_{\xi\xi} = \bar{\tau}_m\sum_{i=1}^{2}\left[\left(m_i^2(c_1 - 1) + \frac{s^2}{\bar{\tau}_m}\right)A_i K_0(m_i r) - \frac{m_i(c_1+1)}{r}A_i K_1(m_i r)\right], \tag{56}$$

$$\bar{\sigma}_{zz} = \bar{\tau}_m\sum_{i=1}^{2}\left[\left(m_i^2\left(c_3 - \frac{\varepsilon_3}{\varepsilon_1}\right) + \frac{\varepsilon_3 s^2}{\varepsilon_1\bar{\tau}_m}\right)A_i K_0(m_i r) - \frac{m_i(c_3+c_4)}{r}A_i K_1(m_i r)\right]. \tag{57}$$

After using the Laplace transform method, the conditions (35) and (36) become

$$\bar{\psi}_1(R, s) = \frac{\theta_0}{s} + \frac{K_1\theta_0^2}{2s} = \bar{G}(s), \qquad \bar{\sigma}_{rr}(R, s) = 0. \tag{58}$$

Substituting Eqs. (52) and (55) in (58), we get

$$\sum_{i=1}^{2}\left(m_i^2 - \frac{s^2}{\bar{\tau}_m}\right)A_i K_0(m_i R) = \frac{\varepsilon_1}{\bar{\tau}_m}\bar{G}(s), \tag{59}$$

$$\sum_{i=1}^{2}\left[\frac{s^2}{\bar{\tau}_m}A_i K_0(m_i R) + \frac{m_i(1-c_1)}{R}A_i K_1(m_i R)\right] = 0. \tag{60}$$

The equation for the field of the Laplace transform relationship (18) gives

$$\bar{\theta} = \frac{\sqrt{2k_1\bar{\psi}_1 + 1} - 1}{K_1}. \tag{61}$$

6 Numerical technique

In the Section 5, the analytical solutions for different physical fields were obtained. In this current section, the distributions of the studied field quantities such as temperature change, displacement, and pressures will be converted into physical time domains. Due to the difficulty of using direct methods for complex relations, a suitable numerical approximation algorithm based on Fourier series expansion [56] will be used to find Laplace transforms. With this proven and efficient algorithm, any function in the Laplace transform domain can be inverted to the time domain using the following easy formula:

$$H(r,t) = e^{\omega\tau}\left(\frac{1}{2}\bar{H}(r,\omega) + \mathrm{Re}\sum_{n=1}^{m}(-1)^n\bar{H}(r,\omega + in\pi/t)\right)/t, \quad (62)$$

where c satisfies the relation $ct \cong 4.7$ [8].

7 Numerical results and discussion

We now offer some numerical findings to demonstrate the influence of varying thermal material characteristics and viscosity parameters on our theoretical results in the preceding section. As an orthotropic thermoelastic material, cobalt was chosen. The characteristics of cobalt are listed in SI units as follows [57,58]:

$$c_{11} = 3.071 \times 10^{11} \quad (\mathrm{N/m}),\ c_{12} = 1.65 \times 10^{11} \quad (\mathrm{N/m}),$$
$$c_{22} = 3.581 \times 10^{11} \quad (\mathrm{N/m}),$$
$$c_{13} = 1.027 \times 10^{11} \quad (\mathrm{N/m}),\ c_{23} = 1.15 \times 10^{11} \quad (\mathrm{N/m}),$$
$$\rho = 8836 \quad (\mathrm{kg/m^3}) \quad ,\theta_0 = 1,$$
$$\beta_{11} = \beta_{22} = 7.04 \times 10^6 \quad (\mathrm{N/m^2K}),$$
$$\beta_{33} = 6.90 \times 10^6 \quad (\mathrm{N/m^2K}),\ T_0 = 298\ \mathrm{K},$$
$$R = 1, \quad C_E = 4.27 \times 10^2 \quad (\mathrm{J/K\ kg}),$$
$$K_0 = 96 \quad (\mathrm{W/m\ K}), \quad K_0^{\star} = 2\,(\mathrm{W/m\ Ks}).$$

Figures 1–12 and Tables 1–4 show the numerical results for different physical fields along the radial distance r. Numerical calculations and discussions can be divided into four cases:

7.1 Effect of temperature-dependent properties of materials

Based on the MGT thermo-viscoelastic theory, the non-dimensional behavior of temperature change, radial

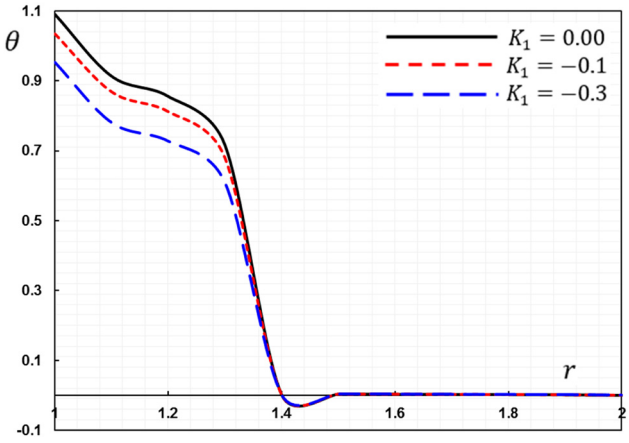

Figure 1: Effect of temperature-dependent thermal conductivity parameter K_1 on the variation in temperature θ.

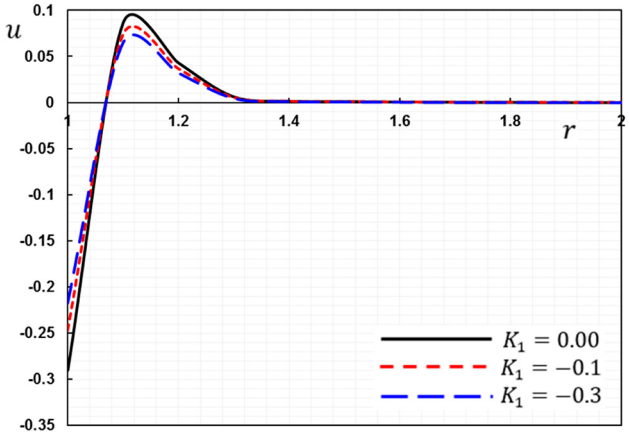

Figure 2: Effect of temperature-dependent thermal conductivity parameter K_1 on the variation in the displacement u.

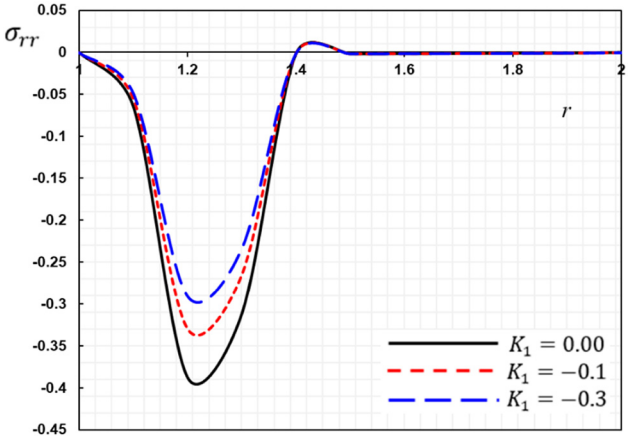

Figure 3: Effect of temperature-dependent thermal conductivity parameter K_1 on the variation in the stress σ_{rr}.

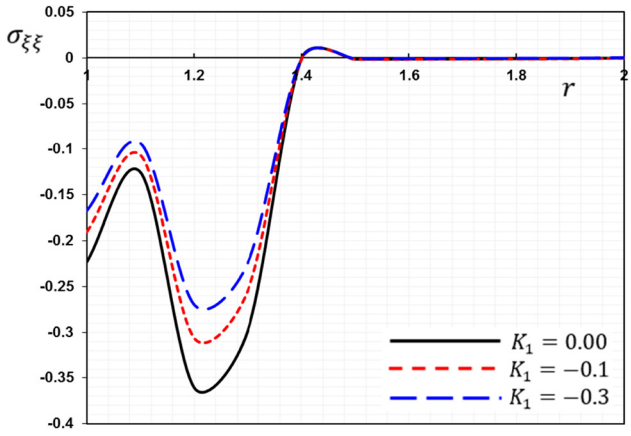

Figure 4: Effect of temperature-dependent thermal conductivity parameter K1 on the variation in the stress $\sigma_{\xi\xi}$.

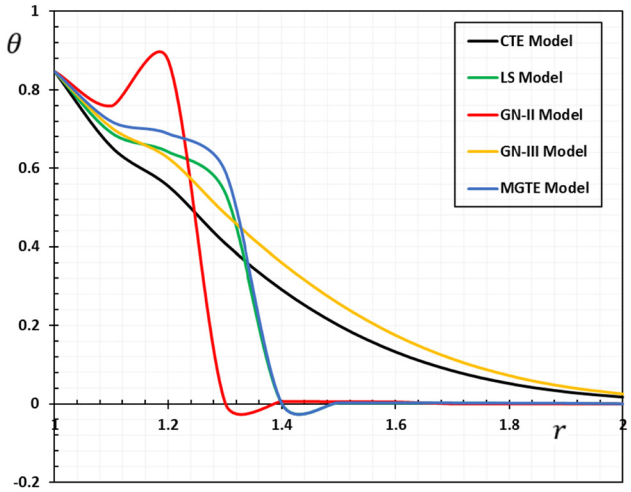

Figure 5: The temperature θ under various models of thermoelasticity.

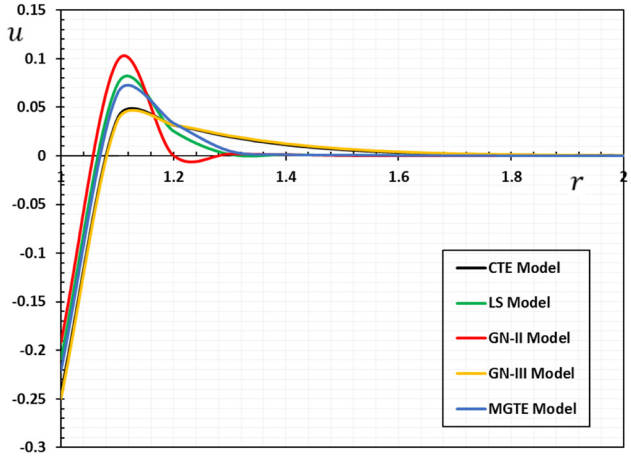

Figure 6: The displacement u under various models of thermoelasticity.

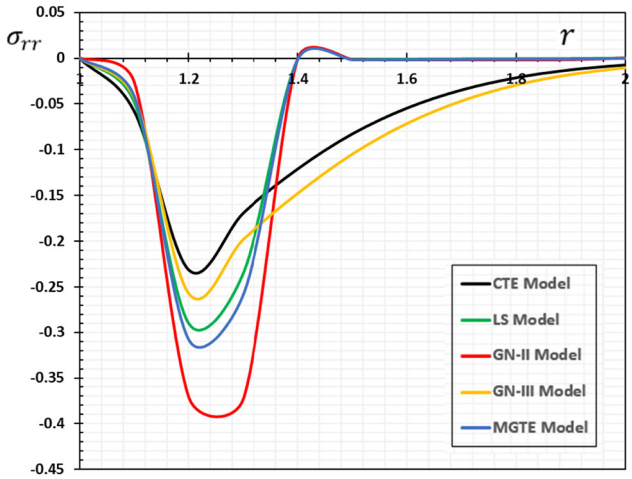

Figure 7: The stress σ_{rr} under various models of thermoelasticity.

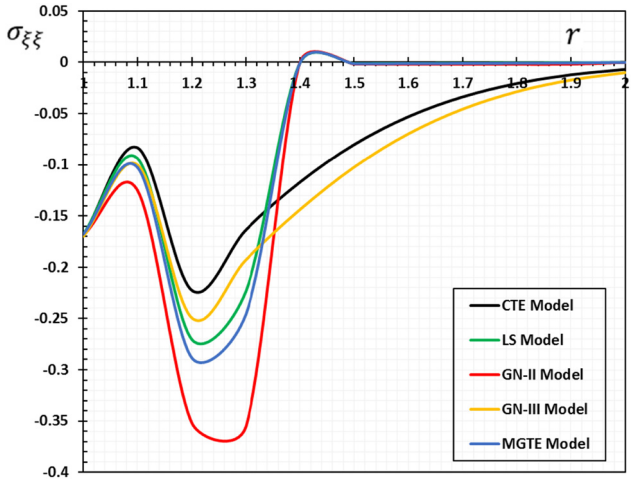

Figure 8: The stress $\sigma_{\xi\xi}$ under various models of thermoelasticity.

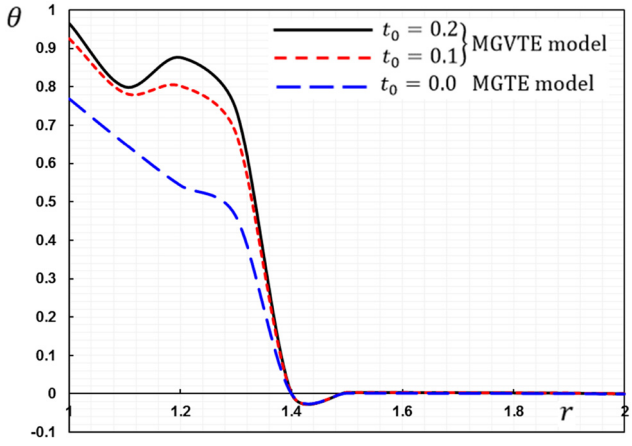

Figure 9: The effect of the viscosity parameter t_0 on the temperature θ.

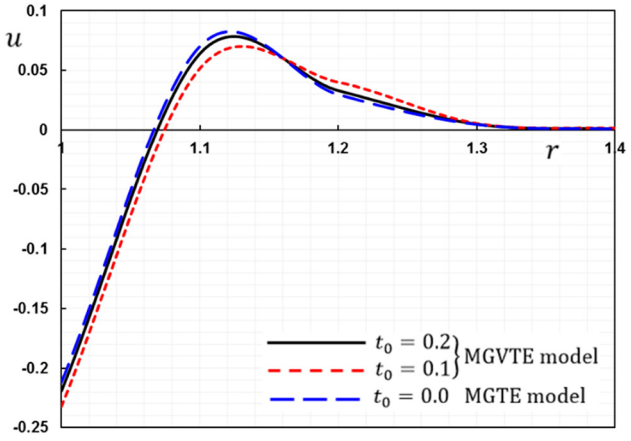

Figure 10: The effect of the viscosity parameter t_0 on the displacement u.

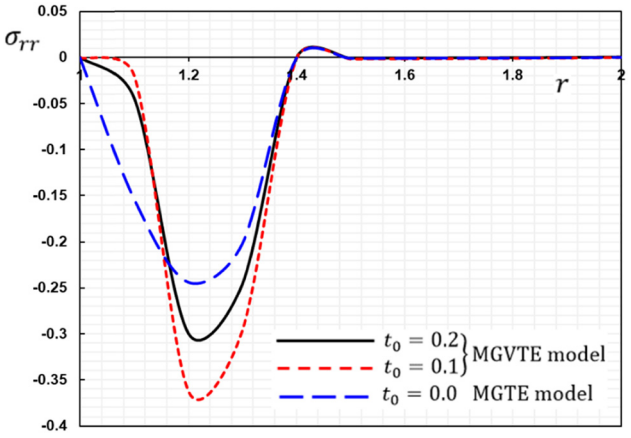

Figure 11: The effect of the viscosity parameter t_0 on the stress σ_{rr}.

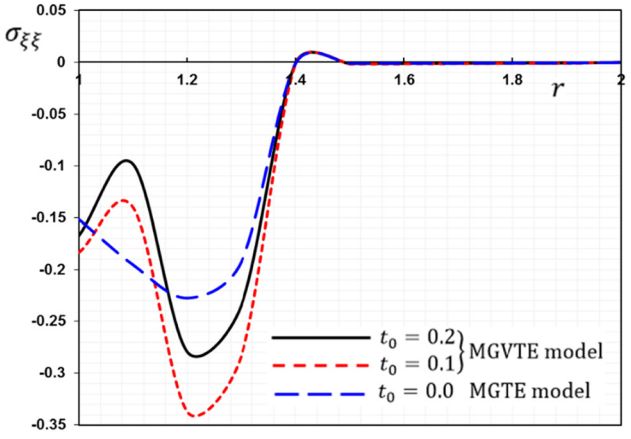

Figure 12: The effect of the viscosity parameter t_0 on the stress $\sigma_{\xi\xi}$.

displacement, and stresses will be studied with various values of the modulus K_1, while relaxation time τ_0 and viscosity parameter t_0 remain fixed. In this study, two cases with different values of the coefficient K_1 responsible for the change in the thermal conductivity coefficient will be considered. The coefficient of thermal conductivity depends on the temperature change at the values $K_1 = -0.5$ and $K_1 = -1.0$, while the thermal conductivity is constant at $K_1 = 0$.

Changes in different physical domains are represented in Figures 1–4. Statistics and numerical results indicate that the coefficient of variation has a significant effect on the behavior of all studied fields. Moreover, the phenomenon of finite propagation velocity of thermal and mechanical waves can be seen within the medium. This is in contrast to the cases where the wave propagation velocity is unlimited in correlated and uncorrelated thermoelastic theories. It is also noted that all the functions concerned have zero value away from the surface and away from the perturbation region. In other words, disturbances occur only in a limited area close to the surface of the inner cavity of the cylinder.

The following relevant facts are also noted:

- From Figure 1, it is clear that the value of temperature change θ varies greatly near the surface, and these differences decrease with time. The amount of the heat wave forward decreases with time and the distance r increases the further away we are from the surface. It is also noticed that the temperature value decreases with a decrease in the coefficient of change of thermal conductivity, K_1. Also, the temperature θ has a non-zero value at a given time in a finite space domain and the disturbances disappear outside this region.
- Figure 2 shows that u displacement changes starting with negative values in all cases and increases continuously to its maximum values, then progressively decreases to zero. Also, as shown in the figure, due to the reduction in parameter K_1, the displacement values u increases during the interval $1.0 \le r \le 1.2$ and decreases during the interval $1.2 \le r \le 1.8$, finally vanishing when $r \ge 1.8$ and reaching a steady state.
- From Figure 3, it can be seen that the thermal stress σ_{rr} starts with a value of zero at the cylindrical cavity $r = 1$, and this corresponds to the boundary conditions imposed on the problem. The stress then decreases rapidly to a minimum negative value at point $r = 1.2$, after which the curves gradually rise after point $r > 1.2$ until finally they reach the steady state. It is further observed from the figure that the variable thermal conductivity parameter K_1 reduces the magnitude of the stress σ_{rr}.
- From Figure 4, it is noticed that the thermal stress $\sigma_{\xi\xi}$ starts in all different cases with negative values and

Table 1: The temperature θ under various models of thermoelasticity

r	CTE	LS	GN-II	GN-III	MGTE
1	0.846921	0.846921	0.846921	0.846921	0.846921
1.1	0.654932	0.690503	0.758602	0.703636	0.719487
1.2	0.554759	0.641783	0.87534	0.626213	0.688071
1.3	0.408722	0.538014	0.0026404	0.484259	0.592585
1.4	0.291459	0.00125336	0.00605685	0.359902	0.00158821
1.5	0.200296	0.00236294	0.00518465	0.256352	0.0029296
1.6	0.132622	0.00219944	0.00487155	0.175099	0.00280005
1.7	0.0845005	0.00184565	−0.00003449	0.114662	0.00241089
1.8	0.05178	0.00147547	0.000026943	0.0720169	0.00196714
1.9	0.0305173	0.00111969	0.000033313	0.0434357	0.00151106
2	0.0173138	0.0000236248	0.000030410	0.025214	0.000028550

Table 2: The displacement u under various models of thermoelasticity

r	CTE	LS	GN-II	GN-III	MGTE
1	−0.244049	−0.217625	−0.19147	−0.249295	−0.220734
1.1	0.0380871	0.0644109	0.0976041	0.0358032	0.0638767
1.2	0.0316999	0.0323285	0.000261826	0.0318542	0.0337479
1.3	0.0197335	0.00467705	0.00190409	0.0207114	0.00500771
1.4	0.0115354	0.00108763	0.00119537	0.0125974	0.00115163
1.5	0.00652219	0.000697273	0.000207207	0.00739418	0.000775617
1.6	0.00361383	0.000417361	0.0000171533	0.00424539	0.000486633
1.7	0.00196812	0.000226149	0.0000102991	0.00239449	0.00027577
1.8	0.001059	0.000102284	0.0000040434	0.00133573	0.000130004
1.9	0.000566941	0.0000038170	0.0000001247	0.000743515	0.0000356673
2	0.000304729	0.0000022295	0.0000000826	0.000417504	0.0000039773

Table 3: The stress σ_{rr} under various models of thermoelasticity

r	CTE	LS	GN-II	GN-III	MGTE
1	0	0	0	0	0
1.1	−0.0578236	−0.04816140	−0.0263679	−0.0430203	−0.0414677
1.2	−0.2317030	−0.290414000	−0.3714220	−0.2578770	−0.3085120
1.3	−0.1687780	−0.234008000	−0.3718680	−0.1978350	−0.2575180
1.4	−0.1207430	−0.000857084	−0.000541784	−0.1475970	−0.000936736
1.5	−0.0823854	−0.001235540	−0.00176446	−0.1045700	−0.00145079
1.6	−0.0542318	−0.001095020	−0.00199776	−0.0711069	−0.00134401
1.7	−0.0343857	−0.000881889	−0.00202190	−0.0463876	−0.00112500
1.8	−0.02098990	−0.000679896	−0.00198624	−0.0290482	−0.000894497
1.9	−0.01233500	−0.000497941	−0.00190793	−0.0174810	−0.000668977
2	−0.00698464	−0.000011173	−0.000011173	−0.0101331	−0.000015662

decreases until it reaches its lowest value at the point $r = 1.1$, after which it gradually increases until it approaches the steady state near zero. It is further shown that the values of $\sigma_{\xi\xi}$ increase as the values of K_1 decrease.

- The curves representing thermal stresses are compressive in some parts of the cylinder and tensile in some other parts. It is noted that the tensile stresses increase with time and are located in the medium, adjacent to the surface of the cylinder, where this agrees with refs. [39,40]. It is also shown that the maximum values of the studied fields occur near the surface of the stromal cavity and decrease in magnitude with increasing radial distance. This phenomenon has been studied in detail in many previous studies, as in ref. [59].

Table 4: The stress $\sigma_{\xi\xi}$ under various models of thermoelasticity

r	CTE	LS	GN-II	GN-III	MGTE
1	0	0	0	0	0
1.1	−0.0578236	−0.0481614	−0.0263679	−0.0430203	−0.04146770
1.2	−0.2317030	−0.2904140	−0.3714220	−0.2578770	−0.30851200
1.3	−0.1687780	−0.2340080	−0.3718680	−0.1978350	−0.25751800
1.4	−0.1207430	−0.000857084	−0.000541784	−0.1475970	−0.000936736
1.5	−0.0823854	−0.001235540	−0.00176446	−0.1045700	−0.001450790
1.6	−0.0542318	−0.001095020	−0.00199776	−0.0711069	−0.001344010
1.7	−0.0343857	−0.000881889	−0.0020219	−0.0463876	−0.00112500
1.8	−0.0209899	−0.000679896	−0.00198624	−0.0290482	−0.000894497
1.9	−0.01233500	−0.000497941	−0.00190793	−0.0174810	−0.000668977
2	−0.00698464	−0.000011173	−0.000042361	−0.0101331	−0.000015662

- From the numerical results, it is clear that the coefficient responsible for the change in the thermal conductivity coefficient has a prominent effect on the distribution of all different fields, which makes the coefficient of the thermal conductivity variable of great importance in many applications, such as the design and maintenance process [60].
- It turns out that different field quantities depend not only on the variables of time and space but also on the parameters of the thermal conductivity change. The phenomenon of finite propagation velocities is also evident in all of these figures [61].

7.2 Comparison of thermoelastic models

In the current subsection case of the study, the change in different fields against distance r will be investigated with different theories of thermoelasticity when the change in thermal conductivity parameter K_1 is constant.

It can be seen that the following models of thermoelasticity can be obtained as special cases of the model presented in this work. The coupled thermoelasticity model (CTE) is extracted from the proposed model when $\tau_0 = K^* = 0$, while the LS model is obtained from the position ($K^* = 0$). In addition, when $\tau_0 = K = 0$, the rate system becomes true of the second type of Green and Naghdi (GN-II) model. Finally, the third type of Green and Naghdi model (GN-III) can be deduced from the equations when the parameter $\tau_0 = 0$.

Comparisons between the different models are represented in Figures 5–8. In addition to the figures, some numerical results are presented in tables (Tables 1–4) for the purpose of easy comparison between different models of thermoelasticity. From the numerical results shown in the figures and tables, the following conclusions can be drawn:

- Thermal parameters τ_0 and K^* have a significant influence on the distributions of field quantities. CTE model and generalized (LS, GN-II, GN-III, and MGTE) theories give very similar results near the cylinder surface, where boundary conditions predominate. The solution is fundamentally different inside the cylinder away from the surface.
- The relaxation time parameter τ_0 and the parameter K^* have a prominent influence on the behavior of the distributions of different physical domains. It is also noted that the values in the case of the CTE model and the generalized models (LS, GN-II, GN-III, and MGTE) are similar in behavior and very close to the surface of the cylinder, where the boundary conditions of the problem are met.
- As we go inside the cylinder, the values of different domains in the case of the CTE theory differ significantly from the values in the case of other generalized theories. The reason for this is that the CTE theory predicts that heat waves propagate at infinite speeds, whereas they only reach finite speeds in the case of the generalized models that have been developed.
- The numerical results show the discrepancy between the predictions of Green and Naghdi's GN-III theory and the predictions of other generalized theories, in addition to the new model MGTE. From Table 1 and Figure 5, it can be seen that the amount of temperature change in the GN-III model is greater than in the case of the MGTE model. It is also shown that the graphs in the LS and MGTE models reflect similar results in the behavior. The reason for the convergence of values in both LS and MGTE is the inclusion of relaxation time in the heat equation.
- The curves representing the change in temperature as well as other physical domains in the case of the GN-II

model are significantly higher compared to the LS and MGTE models.

- The outcomes show that the values of different distributions in the generalized thermoelastic model GN-III differ fundamentally from the values in the thermoelastic model GN-II due to energy dissipation in the first model.
- The deceleration of the temperature decrease is shown in the LS and MGTE models due to the presence of the relaxation coefficient.
- Among the most important conclusions that were obtained from the numerical results and confirm the validity of the results obtained is that the values in the case of the generalized GN-IIII model converge in behavior with the traditional CTE model. It is observed that the results do not fade quickly inside the body in heat distribution, in contrast to other generalized models. This is consistent with what was discussed by Quintanilla [21]. Quintanilla confirmed that the GN-IIII model has the same limitations as the conventional models. This is a major reason for presenting the proposed model in this work.
- Since the relaxation time τ_0 was proposed to be included in Fourier's law, it was found that the temperature distributions as well as other physical quantities in the case of the MGTE model and the LS model follow similar patterns in viscous solids. In general, the curves of both theories are very similar in behavior and convergence but differ only slightly in the amount.

7.3 Effect of the viscoelasticity factors

The only difference between the elastic and viscoelastic substances is that viscoelastic materials have a mechanical relaxation factor (viscosity) t_0, whereas elastic substances do not. Because of the viscosity component, viscoelastic materials have a strain rate that varies over time. When a load is applied and released, pure elastic materials do not lose heat (energy), but a viscoelastic substance does. Viscoelastic materials are used for vibration isolation, noise damping, and shock absorption. They release the heat they received as a result of the energy they absorbed.

The last case of the discussion will show how the temperature change, radial displacement, and the stresses vary with the change in mechanical relaxation duration t_0 which appears in the viscosity term $\tau_m = 1 + t_0\frac{\partial}{\partial t}$ in the fundamental equations. For the purpose of comparison, in numerical computation, the values $K_1 = -0.5$ and $\tau_0 = 0.1$ will be used. The profiles were examined for three different values due to the viscosity t_0.

The MGTE is applied only in this case. In two distinct instances, comparisons are made for the dimensionless physical quantities: (i) in the case of the MGVTE model, we will take $t_0 = 0.1$ and $t_0 = 0.2$ and (ii) in the case of the MGTE model (non-viscosity), we will set $t_0 = 0$. Comparisons for different domains with r are displayed in Figures 5–8. We summarize the following important notes:

- The viscosity factor has a prominent influence on all the studied fields.
- When a substance is deformed, it has both viscous and elastic properties, which is referred to as viscoelasticity. Noticeable viscoelastic influences may be observed in synthetic polymers, wood, and biological tissues, as well as metallic element at elevated temperatures. Even a minor viscoelastic response might have a big impact in a particular situation.
- It can be seen from Figure 9 that the viscosity coefficient tends to increase in temperature. It is also noticed that the temperature distribution curves in the MGVTE theory are larger than those in the case of the MGTE theory.
- It can be seen from Figure 10 the significant effect of the viscosity coefficient t_0 on the values of the displacement distribution. The displacement curves decrease with increasing mechanical relaxation time τ_0. In addition, it was found that the displacement distribution in the case of the MGTE model is greater than in the case of the MGVTE model. With the differences in both theories, the radial displacement distribution curves are similar, as indicated by ref. [40].
- The effect of the viscosity coefficient on the distribution of thermal stresses σ_{rr} and $\sigma_{\xi\xi}$ is clarified in Figures 11 and 12. The figures showed the prominent effect on the thermal stress curves as mentioned in refs [38,41]. It can be seen from the two figures that the absolute values of the stresses increase with the increase in the value of the viscosity parameter.
- Over time, inside the body, the effect of viscosity disappears, away from the surface of the cavity and away from the area of turbulence.
- From the numerical results, it is clear that the linear viscoelastic materials are rheological materials that appear depending on the average loading time temperature. Their response is not only a function of the current entry but also the date of the current and past entry [37,62].

- The effect of the viscosity coefficient on the distribution of thermal stresses σ_{rr} and $\sigma_{\xi\xi}$ was clarified in Figures 11 and 12. The figures showed prominent effect on the thermal stress curves as mentioned in refs [38,41]. It can be seen from the two figures that the absolute values of the stresses increase with the increase in the value of the viscosity parameter.
- From the numerical results, it is clear that the linear viscoelastic materials are rheological materials that appear depending on the average loading time temperature. Their response is not only a function of the current entry but also of the date of the current and past entries [37,62].
- Understanding the viscoelastic properties of polymeric materials is critical for optimizing elastic formulations and mixtures, as well as regulating material handling parameters.
- The results obtained in this subsection are important in the field of viscoelastic materials, for designers of new materials based on them, physicists working in the low-temperature field, as well as those working on hyperbolic viscoelastic theory (MGVTE).

8 Conclusion

In the current work, a new generalized theory of thermo-viscoelasticity is introduced that includes the MGT equation, which allows heat waves to spread at finite velocities. The thermal conductivity equation was derived based on the LS theory and Green–Naghdi theory of thermal elasticity of the third type (GN-III). Thermal and mechanical disturbances of an infinitely viscous anisotropic medium with a cylindrical bore subjected to a time-dependent thermal shock as well as traction-free were investigated. The following observations can be drawn from the previous discussions:

- The change in thermal conductivity plays an important role in raising or lowering the distributions of the studied fields.
- The presence of the viscous term in the fundamental equations plays a significant role in the numerical results and the distribution of various fields.
- Heat waves propagate as waves of finite velocity in the case of MGT's generalized thermoelasticity theory, rather than infinite speed in the viscoelastic medium in the classical elastic model.
- The conduct of the studied fields in the case of GN-III and CTE models is very close to that of the proposed MGTE model. This result displays a significant of taking into account the presented visco-thermoelastic theory.

Those working in the fields of science and engineering, as well as those working on developing the mechanics of viscous solids, can benefit from the results obtained in this work. The method that was used in this research can also be applied to solve a variety of problems in thermodynamics and engineering structures. We also believe that the theoretical results obtained will provide relevant information for scientists and experimental researchers working in this field.

Acknowledgments: Taif University Researches Supporting Project number (TURSP-2020/031), Taif University, Taif, Saudi Arabia.

Funding information: The authors received financial support from Taif University Researchers Supporting Project Number (TURSP-2020/031), Taif University, Taif, Saudi Arabia.

Author contributions: All authors have accepted responsibility for the entire content of this manuscript and approved its submission.

Conflict of interest: The authors state no conflict of interest.

References

[1] Biot MA. Thermoelasticity and irreversible thermodynamics. J Appl Phys. 1956;27(3):240–53.
[2] Lord HW, Shulman Y. A generalized dynamical theory of thermoelasticity. J Mech Phys Solids. 1967;15(5):299–309.
[3] Cattaneo C. A form of heat-conduction equations which eliminates the paradox of instantaneous propagation. Compt Rend. 1958;247:431–3.
[4] Vernotte P. Les paradoxes de la theorie continue de l'equation de lachaleur. Compt Rend. 1958;246:3154–5.
[5] Vernotte P. Some possible complications in the phenomena of thermal conduction. Compt Rend. 1961;252:2190–1.
[6] Muller I. On the entropy inequality. Arch Ration Mech Anal. 1967;26(2):118–41.
[7] Green AE, Lindsay KA. Thermoelasticity. J Elast. 1972;2(1):1–7.
[8] Green AE, Laws N. On the entropy production inequality. Arch Ration Mech Anal. 1972;45(1):47–53.
[9] Chandrasekharaiah DS. Thermoelasticity with second sound: A review. Appl Mech Rev. 1986;39(3):355–76.
[10] Chandrasekharaiah DS. Hyperbolic thermoelasticity: A review of recent literature. Appl Mech Rev. 1998;51(12):705–29.
[11] Tzou DY, Macro-to micro-scale heat transfer: the lagging behavior. Abingdon, UK: Taylor & Francis; 1997.
[12] Hetnarski RB, Ignaczak J. Generalized thermoelasticity. J Therm Stresses. 1999;22(4–5):451–76.

[13] Abouelregal AE, Ahmad H, Gepreeld KA, Thounthong P. Modelling of vibrations of rotating nanoscale beams surrounded by a magnetic field and subjected to a harmonic thermal field using a state-space approach. Eur Phys J Plus. 2021 Mar;136(3):1–23.
[14] Hetnarski RB, Eslami MR, Gladwell GML. Thermal stresses: advanced theory and applications. Vol. 4. New York, NY, USA: Springer; 2009.
[15] Green AE, Naghdi PM. A re-examination of the basic postulates of thermomechanics. Proc R Soc Lond A. 1991;432:171–94
[16] Abouelregal AE, Ahmad H, Yao SW. Functionally graded piezoelectric medium exposed to a movable heat flow based on a heat equation with a memory-dependent derivative. Materials. 2020;13(18):3953.
[17] Abouelregal AE, Ahmad H. Response of thermoviscoelastic microbeams affected by the heating of laser pulse under thermal and magnetic fields. Phys Scr. 2020;95(12):125501. doi: 10.1088/1402-4896/abc03d.
[18] Abouelregal AE, Yao S-W, Ahmad H. Analysis of a functionally graded thermopiezoelectric finite rod excited by a moving heat source. Results Phys. 2020;19:103389.
[19] Abouelregal AE, Ahmad H. Thermodynamic modeling of viscoelastic thin rotating microbeam based on non-Fourier heat conduction. Appl Math Model. 2020;91:973–88.
[20] Abouelregal AE, Moustapha MV, Nofal TA, Rashid S, Ahmad H. Generalized thermoelasticity based on higher-order memory-dependent derivative with time delay. Results in Physics; 2021;20:103705.
[21] Quintanilla R. Moore-Gibson-Thompson thermoelasticity. Math Mech Solids. 2019;24:4020–31.
[22] Dreher M, Quintanilla R, Racke R. Ill-posed problems in thermomechanics. Appl Math Lett. 2009;22:1374–9.
[23] Roy Choudhuri SK. On a thermoelastic three-phase-lag model. J Therm Stresses. 2007;30:231–8.
[24] Lasiecka I, Wang X. Moore–Gibson–Thompson equation with memory, part II: General decay of energy. J Diff Eqns. 2015;259:7610–35.
[25] Marchand R, McDevitt T, Triggiani R. An abstract semigroup approach to the third order Moore–Gibson–Thompson partial differential equation arising in high-intensity ultrasound: structural decomposition, spectral analysis, exponential stability. Math Meth Appl Sci. 2012;35:1896–1929.
[26] Pellicer M, Sola-Morales J. Optimal scalar products in the Moore–Gibson–Thompson equation. Evol Eq Control Theory. 2019;8:203–20.
[27] Thompson PA. Compressible-Fluid Dynamics. New York: McGraw-Hill; 1972.
[28] Quintanilla R. Moore-Gibson-Thompson thermoelasticity with two temperatures. Appl Eng Sci. 2020;1:100006.
[29] Abouelregal AE, Zakaria K, Sirwah MA, Ahmad H, Rashid AF. Viscoelastic initially stressed microbeam heated by an intense pulse laser *via* photo-thermoelasticity with two-phase lag. Int J Mod Phys C. 2022 Jan 14;2250073.
[30] Abouelregal AE, Ahmad H, Nofal TA, Abu-Zinadah H. Thermoviscoelastic fractional model of rotating nanobeams with variable thermal conductivity due to mechanical and thermal loads. Mod Phys Lett B. 2021 Apr 22;2150297.
[31] Abouelregal AE, Ahmad H, Elagan SK, Alshehri NA. Modified Moore–Gibson–Thompson photo-thermoelastic model for a rotating semiconductor half-space subjected to a magnetic field. Int J of Modern Phys C. 2021;32(12):1–26.
[32] Abouelregal AE, Ahmad H, Badr SK, Almutairi B, Almohsen B. Viscoelastic stressed microbeam analysis based on Moore–Gibson–Thompson heat equation and laser excitation resting on Winkler foundation. J Low Freq Noise Vib Active Control. 2021;41(1):1–21.
[33] Abouelregal AE, Ahmad H, Nofal TA, Abu-Zinadah H. Moore–Gibson–Thompson thermoelasticity model with temperature-dependent properties for thermo-viscoelastic orthotropic solid cylinder of infinite length under a temperature pulse. Phys Scrip; 2021;96(10).
[34] Abouelregal AE, Ahmad H, Yahya AM, Saidi A, Alfadil H. Generalized thermoelastic responses in an infinite solid cylinder under the thermoelastic-diffusion model with four lags. Chin J Phys; 2022;76:121–34.
[35] Abouelregal AE, Ahmad H, Yao SW, Abu-Zinadah H. Thermoviscoelastic orthotropic constraint cylindrical cavity with variable thermal properties heated by laser pulse *via* the MGT thermoelasticity model. Open Phys. 2021 Jan 1;19(1):504–18.
[36] Abouelregal AE, Ahmad H, Badr SK, Elmasry Y, Yao SW. Thermo-viscoelastic behavior in an infinitely thin orthotropic hollow cylinder with variable properties under the non-Fourier MGT thermoelastic model. ZAMM-J Appl Math Mech/Zeitschrift für Angew Math Mech; 2022;102(1):1–19.
[37] Kovalenko AD, Karnaukhov VG. A linearized theory of thermoviscoelasticity. Polym Mech. 1972;8(2):194–9.
[38] Drozdov AD. A constitutive model in finite thermoviscoelasticity based on the concept of transient networks. Acta Mech. 1999;133(1–4):13–37.
[39] Alharbi AM, Bayones FS. Generalized magneto-thermo-viscoelastic problem in an infinite circular cylinder in two models subjected to rotation and initial stress. Appl Math Inf Sci. 2018;12(5):1055–66.
[40] Kundu MR, Mukhopadhyay B. A thermoviscoelastic problem of an infinite medium with a spherical cavity using generalized theory of thermoelasticity. Math Comput Model. 2005;41:25–32.
[41] Baksi A, Roy BK, Bera RK. Eigenvalue approach to study the effect of rotation and relaxation time in generalized magneto-thermo-viscoelastic medium in one dimension. Math Comput Model. 2006;44:1069–79.
[42] Mirzaei M. Lord–Shulman nonlinear generalized thermoviscoelasticity of a strip. Int J Struct Stab Dynam. 2020;20(2):2050017.
[43] Kanoria M, Mallik SH. Generalized thermoviscoelastic interaction due to periodically varying heat source with three-phase-lag effect. Eur J Mech A/Solids. 2010;29:695–703.
[44] Ezzat MA. Fractional thermo-viscoelastic response of biological tissue with variable thermal material properties. J Therm Stresses. 2020;43:9.
[45] Ilioushin A, Pobedria BE. Mathematical theory of thermal viscoelasticity. Moscow, Russia: Nauka; 1970.
[46] Zaitoun MW, Chikh A, Tounsi A, Al-Osta MA, Sharif A, Al-Dulaijan SU, et al. Influence of the visco-Pasternak foundation parameters on the buckling behavior of a sandwich functional graded ceramic–metal plate in a hygrothermal environment. Thin-Walled Struct. 2022;170:108549.
[47] Razzaghi MJ, Daemiashkezari M, Abdulfattah AN, Afrouzi HH, Ahmad H. Thermo-hydraulic performance evaluation of turbulent flow and heat transfer in a twisted flat tube: A CFD

approach. Case Stud Therm Eng. 2022 May 13;102107. doi: 10.1016/j.csite.2022.102107
[48] Mudhaffar IM, Tounsi A, Chikh A, Al-Osta MA, Al-Zahrani MM, Al-Dulaijan SU. Hygro-thermo-mechanical bending behavior of advanced functionally graded ceramic metal plate resting on a viscoelastic foundation. Structures. 2021;33:2177–89.
[49] Derdour A, Bouanani A, Kaid N, Mukdasai K, Algelany AM, Ahmad H, et al. Groundwater Potentiality Assessment of Ain Sefra Region in Upper Wadi Namous Basin, Algeria Using Integrated Geospatial Approaches. Sustainability. 2022;14(8):4450.
[50] Refrafi S, Bousahla AA, Bouhadra A, Menasria A, Bourada F, Tounsi A, et al. Effects of hygro-thermo-mechanical conditions on the buckling of FG sandwich plates resting on elastic foundations. Comput Concr. 2020;25(4):311–25.
[51] Sakhri N, Ahmad H, Shatanawi W, Menni Y, Ameur H, Botmart T. Different scenarios to enhance thermal comfort by renewable-ecological techniques in hot dry environment. Case Stud Therm Eng. 2022 Feb 22;101886.
[52] Yilmaz EU, Khodad FS, Ozkan YS, Abazari R, Abouelregal AE, Shaayesteh MT, et al. Manakov model of coupled NLS equation and its optical soliton solutions. J Ocean Eng Sci. 2022 Mar 17.
[53] Eringen AC. Mechanic of continua. New York: John Wiley, Sons. Inc; 1967.
[54] Othman MIA, Abouelregal AE, Said SM. The effect of variable thermal conductivity on an infinite fiber-reinforced thick plate under initial stress. J Mech Mater Struct. 2019;14(2):277–93.
[55] Noda N. Thermal stresses in materials with temperature-dependent properties. In: Hetnarski RB, editor. Thermal Stresses I. North-Holland, Amsterdam: Elsevier; 1986.
[56] Honig G, Hirdes U. A method for the numerical inversion of Laplace transform. J Comp Appl Math. 1984;10:113–32.
[57] Misra JC, Chattopadhyay NC, Samanta SC. Study of the thermoelastic interactions in an elastic half space subjected to a ramp-type heating—a state–space approach. Int J Eng Sci. 1996;34(5):579–96.
[58] Kumar R, Sharma N, Lata P. Thermomechanical interactions due to Hall current in transversely isotropic thermoelastic with and without energy dissipation with two temperatures and rotation. J Solid Mech. 2016;8(4):840–58.
[59] Soleiman A, Abouelregal AE, Ahmad H, Thounthong P. Generalized thermoviscoelastic model with memory dependent derivatives and multi-phase delay for an excited spherical cavity. Phys Scr. 2020;95(11):115708.
[60] Ezzat MA, El-Bary AA. On thermo-viscoelastic infinitely long hollow cylinder with variable thermal conductivity. Microsyst Technol. 2016;23(8):3263–70.
[61] Alzahrani F. The effects of variable thermal conductivity in semiconductor materials photogenerated by a focused thermal shock. Mathematics. 2020;8(8):1230.
[62] Zhai J-J, Kong X-X, Wang L-C. Thermo-viscoelastic response of 3D braided composites based on a novel FsMsFE method. Materials. 2021;14(2):271.